Signal Processing 142 (2018) 388–397

Contents lists available at ScienceDirect

Signal Processing

journal homepage: www.elsevier.com/locate/sigpro

Reduced-complexity direction of arrival estimation with centro-symmetrical arrays and its performance analysis

Feng-Gang Yan[a,b], Bin Cao[c], Shuai Liu[a,*], Ming Jin[a], Yi Shen[b]

[a] Harbin Institute of Technology at Weihai, Weihai 264209, China
[b] Harbin Institute of Technology, Harbin 150001, China
[c] Harbin Institute of Technology at Shenzhen, Shenzhen 518055, China.

ARTICLE INFO

Article history:
Received 19 May 2017
Revised 4 July 2017
Accepted 28 July 2017
Available online 4 August 2017

Keywords:
Direction-of-arrival (DOA) estimation
Real-valued computation
Reduced dimension
Centro-symmetrical array (CSA)
Statistical performance analysis

ABSTRACT

A fast algorithm is proposed to *dramatically* reduce the computational complexity of the multiple signal classification (MUSIC) algorithm for direction-of-arrival (DOA) estimate using a centro-symmetrical array (CSA). The CSA is divided into two sub-arrays and a real matrix is constructed with the covariance matrices of the two sub-arrays and their cross-correlation ones. This real matrix is further regarded as the data covariance one observed by a virtual array which has a real array response, and a novel MUSIC-like cost function is derived accordingly. In the developed method, only real-valued computation is required and the spectral search is compressed into half of the total angular field-of-view. Furthermore, the dimensions of noise subspace and those of search vector are both reduced, leading to about 97% complexity reduction as compare to MUSIC. The non-asymptotic statistical performance of the new DOA estimator is analyzed and a closed-form expression is given to predict the mean square error (MSE) of DOA estimation by the new technique. The effectiveness of the presented approach as well as the theoretical analysis is verified through numerical computer simulations, and it is shown that the proposed method is able to provide good accuracy with low signal-to-noise ratio (SNR) and small numbers of snapshots.

© 2017 Elsevier B.V. All rights reserved.

1. Introduction

Many applications in array signal processing require the determination of the direction of arrivals (DOAs) of different signals impinging from distinct directions on an array of spatially distributed sensors or antennas [1,2]. Numerous DOA estimation methods have been proposed and analyzed in the literature. Among the multiple signal classification (MUSIC) algorithm firstly achieves a so-called super resolution by performing an eigenvalue decomposition (EVD) or a singular value decomposition (SVD) on the array covariance matrix to exploit the orthogonality between the signal- and the noise- subspaces for DOA estimate [3]. Because those two subspaces are as orthogonal to each other as possible when the signal-to-noise ratio (SNR) is sufficiently high, the MUSIC algorithm is able to resolve two sources as closely-spaced as possible [4]. The primary advantage of MUSIC over the other super-resolution techniques is its easy implementation with arbitrary array configurations [5,6]. However, since conventional MUSIC involves a computationally demanding spectral search step, it can be prohibitively expensive in scenarios where real-time processing is required [7].

Great efforts on complexity reduction have been made by avoiding the heavy spectral search step using a sensor array with a special geometry [8] since the specific properties of the array geometry allow a reduction of the degrees of freedom to be estimated [9–11]. In fact, this kind of information has been largely exploited in array detection. For instance, exploiting the centro-hermitian structure for the interference covariance matrix stems from uniform linear array (ULA) or uniformly spaced pulse trains leads to real data vectors and double number of data, followed by better detection and estimation performances [12–14]. For DOA estimation, it is well known that when the array satisfies the rotational invariant property, DOAs can be computed without spectral search by the well-known estimation of signal parameters via rotational invariance technique (ESPRIT) [15]. Another efficient search-free modification of the standard MUSIC is the root-MUSIC algorithm [16], which can be equivalently regarded as a special case of MUSIC with a ULA [17]. Although ESPRIT has a much lower complexity than MUSIC, it sacrifices a significant estimation accuracy on the other hand. Since root-MUSIC generally requires to find the roots of an involved polynomial whose order is about twice that of

* Corresponding author.
E-mail address: liu_shuai_boy@163.com (S. Liu).

http://dx.doi.org/10.1016/j.sigpro.2017.07.033
0165-1684/© 2017 Elsevier B.V. All rights reserved.

the number of sensors, the computational burden of root-MUSIC may be higher than expected [18].

Noting that all of the operations in the standard MUSIC are implemented with expensive complex computations, a unitary MUSIC (U-MUSIC) algorithm is proposed to reduce the complexity with a centro-symmetrical array (CSA), which involves only real-valued arithmetics for both tasks of EVD/SVD and spectral search [19]. Following this idea, a number of other real-valued DOA estimators including U-ESPRIT [20], U-root-MUSIC [21], U-MODE [22] and U-MP [23] are also proposed. Techniques of unitary transformation and forward/backword (FB) averaging [24] are exploited by those methods to transform the complex array covariance matrix to a symmetrical real one, followed by a real-valued subspace decomposition on this symmetrical matrix. It has been shown that U-MUSIC can reduce about 75% computational flops with an improved accuracy as compared to MUSIC [25]. However, it should be noted that U-MUSIC involves a full spectral search and its complexity is in fact still high.

We have developed in [26] another real-valued MUSIC (RV-MUSIC) technique which can be used with arbitrary array geometries. Unlike previous unitary methods, RV-MUSIC exploits a split subspace decomposition on the array covariance matrix with a real-valued subspace composition and it requires a limited spectral search over half of the total angular field-of-view. Therefore, this algorithm has a lower computational burden as compared to U-MUSIC. Nevertheless, the spectral search of RV-MUSIC still requires complex computations, which means that there is in fact a wide space to further reduce the computational complexity.

In this paper, we propose a fast method to *dramatically* reduce the computational complexity of MUSIC using a CSA, in which the CSA is considered as two sub-arrays, and a symmetrical real matrix for real-valued subspace decomposition is obtained by using the covariance matrices of the two sub-arrays and their cross-correlation ones. The developed method only requires real-valued computations and its spectral search is compressed to half. Furthermore, the data dimensions are also reduced, leading to about 97% complexity reduction as compare to the standard MUSIC. As a further development of our previous work in [27], we provide a non-asymptotic statistical performance to give more insights into the new method, and a closed-form expression is derived to predict the mean square error (MSE) of DOA estimation by the new technique. Numerical simulations are applied to verify the effectiveness of the presented approach, which demonstrate that the new method is able to provide good accuracy with low SNRs and small numbers of snapshots.

The remainder of this paper is organized as follows. The signal model for DOA estimation using a CSA is given and some related works are briefly reviewed in Section 2. Section 3 is the main body of this paper, in which the detailed derivations of the proposed method and its extension to two-dimensional (2-D) DOA estimation are described. Section 4 presents the complexity analysis and summary of the proposed method. In Section 5, the statistical performance of the new method is studied and an expression of MSE for DOA estimation by the new technique is given. Numerical simulations are given in Section 6 to demonstrate the effectiveness of our method as well as to verify the theoretical analysis, and the conclusions of this work are summarized in Section 7.

2. Signal model and related works

2.1. Signal model

Assume that there are K narrowband uncorrelated signals with unknown DOAs $\boldsymbol{\Theta} \triangleq \{\theta_1, \theta_2, \ldots, \theta_K\}$ simultaneously impinging from far-field on a linear CSA composed of M sensors. Select the index of the central sensor of the array to be 0 when $M = 2N+1$ (For the case when $M = 2N$, we assume there is a virtual sensor 0 at the center of the array). The $M \times 1$ array output vector can be written as [3–36]

$$\mathbf{x}(t) = \mathbf{A}(\theta)\mathbf{s}(t) + \mathbf{n}(t), \tag{1}$$

where $\mathbf{s}(t)$ is the $K \times 1$ source waveforms vector, $\mathbf{n}(t)$ is the $M \times 1$ additive white Gaussian noise (AWGN) vector,

$$\mathbf{A}(\theta) \triangleq [\mathbf{a}(\theta_1), \mathbf{a}(\theta_2), \ldots, \mathbf{a}(\theta_K)] \tag{2}$$

is the $M \times K$ array response matrix and

$$\mathbf{a}(\theta_k) \triangleq \left[\xi_k^{-x_N}, \xi_k^{-x_{N-1}}, \ldots, \xi_k^{-x_1}, \xi_k^{0}, \xi_k^{x_1}, \ldots, \xi_k^{x_{N-1}}, \xi_k^{x_N}\right]^T \tag{3}$$

is the $M \times 1$ steering vector, $\xi_k \triangleq e^{-j \cdot \frac{2\pi}{\lambda} \cdot \sin\theta_k}$, $k = 1, 2, \ldots, K$ with $x_i, i = 1, \ldots, N-1, N$ denoting the coordinates of right-side sensors. In addition, $j \triangleq \sqrt{-1}$, λ is center wavelength and $(\cdot)^T$ is transpose. It is assumed that $s_k(t), k = 1, 2, \ldots, K$ are uncorrelated with each other, $\mathbf{s}(t)$ and $\mathbf{n}(t)$ randomly distributed such that

$$E\left[\mathbf{n}(t)\mathbf{n}^T(t)\right] = \mathbf{0} \tag{4-1}$$

$$E\left[\mathbf{n}(t)\mathbf{n}^H(t)\right] = \sigma_n^2\mathbf{I} \tag{4-2}$$

$$E\left[\mathbf{s}(t)\mathbf{s}^T(t)\right] = \mathbf{0} \tag{4-3}$$

$$E\left[\mathbf{s}(t)\mathbf{s}^H(t)\right] = \mathbf{R}_s \tag{4-4}$$

$$E\left[\mathbf{s}(t)\mathbf{n}^H(t)\right] = \mathbf{0}, \tag{4-5}$$

where $\mathbf{R}_s$ is a diagonal real matrix.

With the above statistical assumptions, the covariance matrix of the array received data can be written as

$$\mathbf{R} \triangleq \mathrm{E}\left[\mathbf{x}(t)\mathbf{x}^H(t)\right] = \mathbf{A}\mathbf{R}_s\mathbf{A}^H + \sigma_n^2\mathbf{I}. \tag{5}$$

The EVD of $\mathbf{R}$ can be expressed as

$$\mathbf{R} = \mathbf{S}\boldsymbol{\Lambda}_s\mathbf{S}^H + \mathbf{G}\boldsymbol{\Lambda}_n\mathbf{G}^H, \tag{6}$$

where $\mathbf{S}$ and $\mathbf{G}$ are the so-called signal- and noise- subspace matrices, respectively. For practical situations, the theoretical $\mathbf{R}$ in (5) is unavailable, and it is usually estimated by L snapshots of the array received data as follows:

$$\widehat{\mathbf{R}} = \frac{1}{L}\sum_{t=1}^{L}\mathbf{x}(t)\mathbf{x}^H(t). \tag{7}$$

Therefore, the subspace decomposition is in fact given by

$$\widehat{\mathbf{R}} = \widehat{\mathbf{S}}\widehat{\boldsymbol{\Lambda}}_s\widehat{\mathbf{S}}^H + \widehat{\mathbf{G}}\widehat{\boldsymbol{\Lambda}}_n\widehat{\mathbf{G}}^H. \tag{8}$$

2.2. Related works

Using $\mathrm{span}(\mathbf{S}) \perp \mathrm{span}(\mathbf{G})$ and $\mathrm{span}(\mathbf{S}) = \mathrm{span}(\mathbf{A})$, the conventional MUSIC algorithm [3] suggests to estimate source DOAs by spectral search as follows

$$\min_{\theta} \; f_{\mathrm{MUSIC}}(\theta) \triangleq \|\mathbf{a}^H(\theta)\widehat{\mathbf{G}}\|^2, \quad \text{s.t. } \theta \in \left[-\frac{\pi}{2}, \frac{\pi}{2}\right]. \tag{9}$$

One of the most important advantages of the MUSIC algorithm is its easy implementation with arbitrary array configurations. However, since MUSIC involves a tremendous spectral search step, it is computationally expensive for real-time applications.

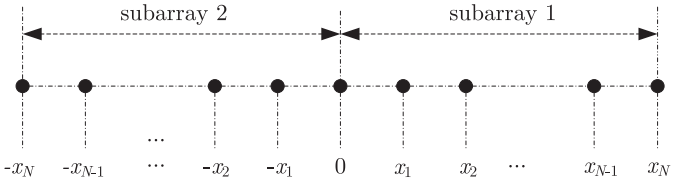

Fig. 1. Subarray selection from a linear CSA with $M = 2N + 1$ sensors.

For MUSIC, both subspace decomposition and spectral search require complex-valued computations. To realize real-valued computations, the U-MUSIC [19] technique transforms the standard MUSIC to a real-valued function as

$$\min_{\theta} \; f_{\text{U-MUSIC}}(\theta) \triangleq \|\mathbb{b}^T(\theta)\widehat{\mathbb{G}}_1\|^2, \quad \text{s.t. } \theta \in \left[-\frac{\pi}{2}, \frac{\pi}{2}\right], \tag{10}$$

where $\mathbb{b}(\theta) \in \mathbb{R}^{M\times 1}$ and $\widehat{\mathbb{G}}_1 \in \mathbb{R}^{M\times(M-K)}$ are real vector and matrix, respectively. The U-MUSIC algorithm can save about 75% complexity as compared to MUSIC.

We have proposed another real-valued RV-MUSIC estimator which exploited a real-valued subspace decomposition (see [26] for detailed illustrations) to limit the exhaustive spectral search of MUSIC to half of the angular field-of-view as

$$\min_{\theta} \; f_{\text{RV-MUSIC}}(\theta) \triangleq \|\mathbf{a}^H(\theta)\widehat{\mathbb{G}}_2\|^2, \quad \text{s.t. } \theta \in \left[-\frac{\pi}{2}, 0\right] \text{ or } \theta \in \left[0, \frac{\pi}{2}\right], \tag{11}$$

where $\widehat{\mathbb{G}}_2 \in \mathbb{R}^{M\times(M-2K)}$ is a real noise orthogonal matrix. Similar to U-MUSIC, RV-MUSIC is able to reduce more than 75% complexity as compared to MUSIC.

3. The proposed algorithm

Divide the CSA into two subarrays along its center position, where the central sensor is shared by the two subarrays (the center sensor is virtual if M is an even number), which is shown in Fig. 1 for more clear illustration. Because the CSA is composed of $M = 2N + 1$ sensors, there are $N + 1$ elements in each subarray. Thus, both the output vectors of the two subarrays are of reduced dimensions $(N + 1) \times 1$, which can be written as

$$\mathbf{x}_1(t) = \mathbf{A}_1(\theta)\mathbf{s}(t) + \mathbf{n}_1(t) \tag{12-1}$$

$$\mathbf{x}_2(t) = \mathbf{A}_2(\theta)\mathbf{s}(t) + \mathbf{n}_2(t), \tag{12-2}$$

where $\mathbf{A}_1(\theta)$ and $\mathbf{A}_1(\theta)$ are the array responses of the two subarrays. To facilitate the representation, let $\mathbf{A}_1 \triangleq \mathbf{A}_1(\theta)$ and $\mathbf{A}_2 \triangleq \mathbf{A}_2(\theta)$. Due to centro-symmetrical structure, the array response matrices of the two sub-arrays can be written as

$$\mathbf{A}_1 = \begin{bmatrix} \xi_1^0 & \xi_2^0 & \cdots & \xi_K^0 \\ \xi_1^{x_1} & \xi_2^{x_1} & \cdots & \xi_K^{x_1} \\ \vdots & \vdots & \ddots & \vdots \\ \xi_1^{x_N} & \xi_2^{x_N} & \cdots & \xi_K^{x_N} \end{bmatrix}, \tag{13-1}$$

$$\mathbf{A}_2 = \begin{bmatrix} \xi_1^0 & \xi_2^0 & \cdots & \xi_K^0 \\ \xi_1^{-x_1} & \xi_2^{-x_1} & \cdots & \xi_K^{-x_1} \\ \vdots & \vdots & \ddots & \vdots \\ \xi_1^{-x_N} & \xi_2^{-x_N} & \cdots & \xi_K^{-x_N} \end{bmatrix}. \tag{13-2}$$

Therefore, we have $\mathbf{A}_1 = \mathbf{A}_2^*$. The covariance matrix of subarray 1 is given by

$$\begin{aligned} \mathbf{R}_{11} &\triangleq E\left[\mathbf{x}_1(t)\mathbf{x}_1^H(t)\right] \\ &= \mathbf{A}_1 E\left[\mathbf{s}(t)\mathbf{s}^H(t)\right]\mathbf{A}_1^H + E\left[\mathbf{n}_1(t)\mathbf{n}_1^H(t)\right] \\ &= \mathbf{A}_1\mathbf{R}_s\mathbf{A}_1^H + \sigma_n^2\mathbf{I}. \end{aligned} \tag{14}$$

Using the fact $\mathbf{A}_1 = \mathbf{A}_2^*$, the covariance matrix of subarray 2 can be written as

$$\begin{aligned} \mathbf{R}_{22} &\triangleq E\left[\mathbf{x}_2(t)\mathbf{x}_2^H(t)\right] \\ &= \mathbf{A}_2 E\left[\mathbf{s}(t)\mathbf{s}^H(t)\right]\mathbf{A}_2^H + E\left[\mathbf{n}_2(t)\mathbf{n}_2^H(t)\right] \\ &= \mathbf{A}_1^*\mathbf{R}_s\mathbf{A}_1^T + \sigma_n^2\mathbf{I}. \end{aligned} \tag{15}$$

Since $\mathbf{n}_1(t)$ and $\mathbf{n}_2(t)$ are independent AWGNs, the cross-covariance matrix of the two sub-arrays can be computed by

$$\begin{aligned} \mathbf{R}_{12} &\triangleq E\left[\mathbf{x}_1(t)\mathbf{x}_2^H(t)\right] \\ &= \mathbf{A}_1 E\left[\mathbf{s}(t)\mathbf{s}^H(t)\right]\mathbf{A}_2^H + E\left[\mathbf{n}_1(t)\mathbf{n}_2^H(t)\right] \\ &= \mathbf{A}_1\mathbf{R}_s\mathbf{A}_1^T \end{aligned} \tag{16}$$

$$\begin{aligned} \mathbf{R}_{21} &\triangleq E\left[\mathbf{x}_2(t)\mathbf{x}_1^H(t)\right] \\ &= \mathbf{A}_2 E\left[\mathbf{s}(t)\mathbf{s}^H(t)\right]\mathbf{A}_1^H + E\left[\mathbf{n}_2(t)\mathbf{n}_1^H(t)\right] \\ &= \mathbf{A}_1^*\mathbf{R}_s\mathbf{A}_1^H, \end{aligned} \tag{17}$$

where the fact $\mathbf{A}_1 = \mathbf{A}_2^*$ as well as $E\left[\mathbf{n}_1(t)\mathbf{n}_2^H(t)\right] = \mathbf{0}$ is used in the last lines of (16) and (17). From (14)–(17), one can easily conclude that $\mathbf{R}_{11} = \mathbf{R}_{22}^*$ and $\mathbf{R}_{12} = \mathbf{R}_{21}^*$. It is worth noting that all the four matrices $\mathbf{R}_{11}$, $\mathbf{R}_{22}$, $\mathbf{R}_{12}$ and $\mathbf{R}_{21}$ share the same reduced dimensions $(N + 1) \times (N + 1)$ as compared to $\mathbf{R}$, which is of dimensions $(2N + 1) \times (2N + 1)$.

Now, we define a new $(N + 1) \times (N + 1)$ matrix $\mathbb{R}$ as follows:

$$\mathbb{R} \triangleq \mathbf{R}_{11} + \mathbf{R}_{22} + \mathbf{R}_{12} + \mathbf{R}_{21}.$$

Using (14)–(17), $\mathbb{R}$ can be further expressed by

$$\begin{aligned} \mathbb{R} &= \mathbf{A}_1^*\mathbf{R}_s\mathbf{A}_1^H + \mathbf{A}_1\mathbf{R}_s\mathbf{A}_1^H + \sigma_n^2\mathbf{I} \\ &\quad + \mathbf{A}_1\mathbf{R}_s\mathbf{A}_1^T + \mathbf{A}_1^*\mathbf{R}_s\mathbf{A}_1^T + \sigma_n^2\mathbf{I} \\ &= (\mathbf{A}_1^* + \mathbf{A}_1)\mathbf{R}_s\mathbf{A}_1^H + (\mathbf{A}_1 + \mathbf{A}_1^*)\mathbf{R}_s\mathbf{A}_1^T + 2\sigma_n^2\mathbf{I} \\ &= (\mathbf{A}_1 + \mathbf{A}_1^*)\mathbf{R}_s(\mathbf{A}_1 + \mathbf{A}_1^*)^T + 2\sigma_n^2\mathbf{I} \\ &\triangleq \mathbb{A}\mathbf{R}_s\mathbb{A}^T + 2\sigma_n^2\mathbf{I}, \end{aligned} \tag{18}$$

where

$$\mathbb{A} \triangleq \mathbf{A}_1 + \mathbf{A}_1^* = 2\text{Re}(\mathbf{A}),$$

and $\text{Re}(\cdot)$ stands for the real part of the embrace matrix. Because both $\mathbb{A}$ and $\mathbf{R}_s$ are real matrices, it follows directly from (18) that $\mathbb{R}$ must be a real matrix. Comparing (18) with (14)–(17), it can be easily concluded that $\mathbb{R}$ can be regarded as the covariance matrix of the received data by an array with response matrix $\mathbb{A}$. Therefore, we can similarly exploit the MUSIC algorithm with $\mathbb{R}$ instead of $\mathbf{R}$ to find source DOAs, which can result in a significantly reduced complexity as compared to the standard MUSIC.

According to (7) and (14)–(17), the theoretical $\mathbb{R}$ can be estimated in practice by using L snapshots of the received data of the two subarrays as

$$\begin{aligned} \widehat{\mathbb{R}}_L &\triangleq \widehat{\mathbf{R}}_{11} + \widehat{\mathbf{R}}_{22} + \widehat{\mathbf{R}}_{12} + \widehat{\mathbf{R}}_{21} \\ &= \frac{1}{L}\sum_{t=1}^{L}\left[\mathbf{x}_1(t)\mathbf{x}_1^H(t) + \mathbf{x}_2(t)\mathbf{x}_2^H(t)\right] \\ &\quad + \frac{1}{L}\sum_{t=1}^{L}\left[\mathbf{x}_1(t)\mathbf{x}_2^H(t) + \mathbf{x}_2(t)\mathbf{x}_1^H(t)\right] \\ &= \frac{1}{L}\sum_{t=1}^{L}\left[\mathbf{x}_1(t) + \mathbf{x}_2(t)\right]\left[\mathbf{x}_1(t) + \mathbf{x}_2(t)\right]^H. \end{aligned} \tag{19}$$

For a finite number of snapshot, i.e., $L<\infty$, the additional AWGN noises $\widehat{\mathbf{n}}_1(t)$ and $\widehat{\mathbf{n}}_2(t)$ does not satisfy the statistical assumptions in (4) any more. Therefore, we may have $\widehat{\mathbf{R}}_{11}\neq\widehat{\mathbf{R}}_{22}^*$ and $\widehat{\mathbf{R}}_{12}\neq\widehat{\mathbf{R}}_{21}^*$, and consequently, $\widehat{\mathbb{R}}_{\mathrm{L}}$ may be a complex matrix in practice such that

$$\mathrm{Im}\big(\widehat{\mathbb{R}}_{\mathrm{L}}\big)\neq\mathbf{0}, \tag{20}$$

where $\mathrm{Im}(\cdot)$ denotes the imaginary part of the embrace matrix. With the assumption $K<N+1$, we can perform the EVD on $\widehat{\mathbb{R}}_{\mathrm{L}}$ as follows:

$$\widehat{\mathbb{R}}_{\mathrm{L}}=\widehat{\mathcal{S}}\widehat{\mathbf{\Omega}}_s\widehat{\mathcal{S}}^H+\widehat{\mathcal{N}}\widehat{\mathbf{\Omega}}_n\widehat{\mathcal{N}}^H, \tag{21}$$

where subscripts s and n stand for the signal- and the noise- subspaces, respectively, and $\mathbf{\Omega}_s$ and $\mathbf{\Omega}_n$ are two diagonal matrices composed of the K significant- and the $N+1-K$ zero- eigenvalues of $\widehat{\mathbb{R}}_{\mathrm{L}}$, respectively. Note that $\widehat{\mathcal{S}}$, $\widehat{\mathcal{N}}$, $\widehat{\mathbf{\Omega}}_s$ and $\widehat{\mathbf{\Omega}}_n$ are all complex matrices. Theoretically, using the orthogonality between $\mathrm{span}(\mathbb{A})$ and $\mathrm{span}(\mathcal{N})$, we can exploit $\widehat{\mathcal{N}}$ to construct a MUSIC-like cost function for fast DOA estimate. We name the new estimator as reduced-dimension real-valued MUSIC (RDRV-MUSIC) and its *exact* cost function is given by

$$\begin{aligned}&\min_{\theta}\ f^{exact}_{\mathrm{RDRV-MUSIC}}(\theta)=\|\mathbb{a}^T(\theta)\widehat{\mathcal{N}}\|^2,\\&\text{s.t. }\theta\in\left[-\frac{\pi}{2},0\right]\ or\ \theta\in\left[0,\frac{\pi}{2}\right],\end{aligned} \tag{22}$$

where $\mathbb{a}(\theta)$ is a $(N+1)\times1$ real vector which is given by

$$\mathbb{a}(\theta)\triangleq\begin{bmatrix}1\\ \cos\left(\frac{2\pi}{\lambda}\cdot x_1\cdot\sin\theta\right)\\ \cos\left(\frac{2\pi}{\lambda}\cdot x_2\cdot\sin\theta\right)\\ \vdots\\ \cos\left(\frac{2\pi}{\lambda}\cdot x_N\cdot\sin\theta\right)\end{bmatrix}.$$

Nevertheless, expensive complex computations are involved in the search step of (22) because $\widehat{\mathcal{N}}$ is a complex matrix.

To further realize complete real-valued computations, we omit the imaginary part of $\widehat{\mathbb{R}}_{\mathrm{L}}$ in practice to obtain an approximated estimation of $\mathbb{R}$ as follows:

$$\widehat{\mathbb{R}}\approx\mathrm{Re}\big(\widehat{\mathbb{R}}_{\mathrm{L}}\big), \tag{23}$$

whose EVD can be written as

$$\widehat{\mathbb{R}}=\widehat{\mathbb{S}}\widehat{\mathbb{W}}_s\widehat{\mathbb{S}}^T+\widehat{\mathbb{G}}\widehat{\mathbb{W}}_n\widehat{\mathbb{G}}^T, \tag{24}$$

where $\widehat{\mathbb{S}}$ and $\widehat{\mathbb{G}}$ are the signal- and noise- matrices, respectively, $\widehat{\mathbb{W}}_s$ and $\widehat{\mathbb{W}}_n$ are two diagonal matrices composed of the K significant- and the $N+1-K$ zero- eigenvalues of $\widehat{\mathbb{R}}$, respectively. Since $\widehat{\mathbb{R}}$ is real, $\widehat{\mathbb{S}}$, $\widehat{\mathbb{W}}_s$, $\widehat{\mathbb{G}}$ and $\widehat{\mathbb{W}}_n$ are all real matrices accordingly. With the real matrix $\widehat{\mathbb{G}}$ computed by the EVD of $\widehat{\mathbb{R}}$, the proposed RDRV-MUSIC estimator is given by

$$\begin{aligned}&\min_{\theta}\ f_{\mathrm{RDRV-MUSIC}}(\theta)\approx\|\mathbb{a}^T(\theta)\widehat{\mathbb{G}}\|^2,\\&\text{s.t. }\theta\in\left[-\frac{\pi}{2},0\right]\ or\ \theta\in\left[0,\frac{\pi}{2}\right].\end{aligned} \tag{25}$$

Remark 1. It can be concluded by comparing (19) to (23) that using $\widehat{\mathbb{R}}$ instead of $\widehat{\mathbb{R}}_L$ means that $\mathcal{O}(1/L)$ are neglected in practice. However, it is to be shown by theoretical performance analysis in Section 5 and simulations in Section 6 that this dropped error does not effect the proposed algorithm remarkably, and new method performs well with a small L.

Since $\mathbb{a}(\theta)$ and $\mathbb{G}$ are real, we must have $\|\mathbb{a}^T(\theta_k)\widehat{\mathbb{G}}\|^2=0$ and $\|\mathbb{a}^T(-\theta_k)\widehat{\mathbb{G}}\|^2=0$, where θ_k, $k\in[1,K]$ are unknown DOAs. Therefore, the minima of $f_{\mathrm{RDRV\text{-}MUSIC}}(\theta)$ over only half of total angular field-of-view, i.e., $[-\pi/2,0]$ or $[0,\pi/2]$ are either the K true DOAs or their images. This means that we can search over $[-\pi/2,0]$ or $[0,\pi/2]$ to obtain Q candidate angles $\mathbf{\Gamma}\triangleq\{\widehat{\theta}_1,\widehat{\theta}_2,\cdots,\widehat{\theta}_Q\}$. According to the symmetries between the true DOAs and their mirror angles, the K source DOAs can be finally selected from $\mathbf{\Gamma}$ and $-\mathbf{\Gamma}=\{-\widehat{\theta}_1,-\widehat{\theta}_2,\cdots,-\widehat{\theta}_Q\}$ [6,26].

Capon's minimum variance distortionless response (MVDR) beamfomer [28] is exploited here to select the K true DOAs among $\mathbf{\Gamma}$ and $-\mathbf{\Gamma}$. Since the steering vector belongs to the signal subspace only at the true signal incident angles, the MVDR spectral amplitudes responding to the true DOAs must be much smaller than those associated with symmetrical mirrors. On the other hand, as the number of the true DOAs, i.e., K, is known in advance, the K true DOAs can be easily selected among the candidate angles by

$$\widehat{\mathbf{\Theta}}=\{\widehat{\theta}_1,\widehat{\theta}_2,\cdots,\widehat{\theta}_K\}=\arg\min_{\theta\in\{\mathbf{\Gamma},-\mathbf{\Gamma}\}}f_{\mathrm{MVDR}}(\theta), \tag{26}$$

where

$$f_{\mathrm{MVDR}}(\theta)\triangleq\|\mathbf{c}^H(\theta)\widehat{\mathbf{R}}_{11}^{-1}\mathbf{c}(\theta)\|.$$

Here, $\mathbf{c}(\theta)\triangleq\left[\xi^0,\xi^1,\ldots,\xi^N\right]^T$ denotes the steering vector of subarray 1. Although using MVDR to exclude the symmetrical mirror DOAs means that there is an additional step for computing the MVDR spectral involved in the proposed estimator, the complexity of this step is substantially lower since we only need to compute the product $\|\mathbf{c}^H(\theta)\widehat{\mathbf{R}}_{11}^{-1}\mathbf{c}(\theta)\|$ for at most $2K$ spectral points.

Remark 2. For a true DOA θ_k, $f_{\mathrm{RDRV\text{-}MUSIC}}(\theta)$ must show two symmetrical peaks at angles θ_k and $-\theta_k$ simultaneously. Therefore, for K true DOAs, there are at most K peaks in $f_{\mathrm{RDRV\text{-}MUSIC}}(\theta)$ over half of the angular field-of-view. This happens if and only if any two of the K true DOAs are not symmetrical. Oppositely, $f_{\mathrm{RDRV\text{-}MUSIC}}(\theta)$ can generate at least $\lfloor K/2\rfloor$ peaks over half of the angular field-of-view, where $\lfloor\cdot\rfloor$ denotes round down to integer operation. This happens if and only if all the K true DOAs are paired symmetrical themselves. In other words, the number of candidate angels, i.e., Q satisfies $\lfloor K/2\rfloor\le Q\le K$.

Although we elaborate the proposed algorithm in the case of the one-dimensional (1-D) far-field model with a linear CSA, it can be directly extended to estimate the 2-D signal directions $(\mathbf{\Theta},\mathbf{\Phi})\triangleq\{(\theta_1,\phi_1),(\theta_2,\phi_2)\ldots,(\theta_K,\phi_K)\}$ with a plane CSA. To show this clearly, we take a $X-Y$ plane CSA for example, which are composed of $M=2N+1$ sensors with N sensors located in both the first- and the third- quadrants symmetrically. Due to the centro-symmetrical geometrical, we can similarly divide the 2-D CSA along its central position to obtain two subarrays, as shown clearly in Fig. 2. Introducing two electrical angles $\mu\triangleq\cos\theta\cos\phi$ and $\psi\triangleq\cos\theta\sin\phi$, the 2-D array response matrices of the two subarrays $\mathbf{A}_1\triangleq\mathbf{A}_1(\mu,\psi)$ and $\mathbf{A}_2\triangleq\mathbf{A}_2(\mu,\psi)$ can be expressed as

$$\mathbf{A}_1=\begin{bmatrix}1&\cdots&1\\ e^{j\cdot\frac{2\pi}{\lambda}\cdot(x_1\mu+y_1\psi)}&\cdots&e^{j\cdot\frac{2\pi}{\lambda}\cdot(x_N\mu_K+y_N\psi_K)}\\ \vdots&\ddots&\vdots\\ e^{j\cdot\frac{2\pi}{\lambda}\cdot(x_N\mu+y_N\psi)}&\cdots&e^{j\cdot\frac{2\pi}{\lambda}\cdot(x_N\mu_K+y_N\psi_K)}\end{bmatrix}$$

$$\mathbf{A}_2=\begin{bmatrix}1&\cdots&1\\ e^{-j\cdot\frac{2\pi}{\lambda}\cdot(x_1\mu+y_1\psi)}&\cdots&e^{-j\cdot\frac{2\pi}{\lambda}\cdot(x_N\mu_K+y_N\psi_K)}\\ \vdots&\ddots&\vdots\\ e^{-j\cdot\frac{2\pi}{\lambda}\cdot(x_N\mu+y_N\psi)}&\cdots&e^{-j\cdot\frac{2\pi}{\lambda}\cdot(x_N\mu_K+y_N\psi_K)}\end{bmatrix},$$

where (x_i,y_i), $i\in[1,N]$ are the coordinates of the ith sensor in the first quadrant. Clearly, $\mathbf{A}_1(\mu,\psi)=\mathbf{A}_2^*(\mu,\psi)$ holds. Thus, we can similarly find the real noise matrix $\mathbb{G}$ computed from the real covariance matrix $\mathbb{R}$, and the Q 2-D candidate signal DOAs $\mathbf{\Gamma}$ can be finally estimated by

$$\min_{(\mu,\psi)}\ f_{\mathrm{2D-RDRV-MUSIC}}(\mu,\psi)\triangleq\|\mathbb{a}^T(\mu,\psi)\widehat{\mathbb{G}}\|^2$$

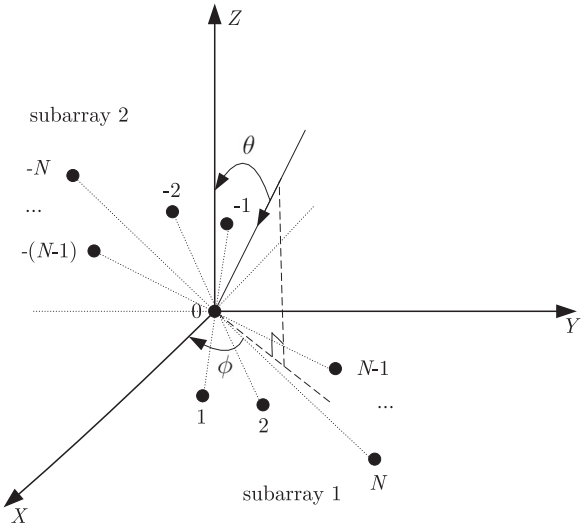

Fig. 2. Subarray selection from a plane CSA with $M = 2N + 1$ sensors.

$$\text{s.t.} \quad (\mu, \psi) \in [-1, 0] \times [-1, 1] \text{ or}$$
$$(\mu, \psi) \in [0, 1] \times [-1, 1] \text{ or}$$
$$(\mu, \psi) \in [-1, 1] \times [-1, 0] \text{ or}$$
$$(\mu, \psi) \in [-1, 1] \times [0, 1],$$

where $\mathbb{a}(\mu, \psi)$ is a $(N+1) \times 1$ real vector, given by

$$\mathbb{a}(\mu, \psi) \triangleq \begin{bmatrix} 1 \\ \cos\left[\frac{2\pi}{\lambda} \cdot (x_1\mu + y_1\psi)\right] \\ \vdots \\ \cos\left[\frac{2\pi}{\lambda} \cdot (x_N\mu + y_N\psi)\right] \end{bmatrix}.$$

The K true 2-D DOAs can be similarly selected from $\mathbf{\Gamma}$ and $-\mathbf{\Gamma}$ by minimizing the product $\|\mathbf{c}^H(\mu, \psi)\widehat{\mathbf{R}}_{11}^{-1}\mathbf{c}(\mu, \psi)\|$, where $\mathbf{c}(\mu, \psi)$ denotes the steering vector of subarray 1.

Detailed steps for implementing the presented RDRV-MUSIC algorithm are summarized in Algorithm 1.

Algorithm 1 The proposed RDRV-MUSIC algorithm.

Require: $\{\widehat{\mathbf{x}}_1(t)\}_{t=1}^L$ and $\{\widehat{\mathbf{x}}_2(t)\}_{t=1}^L$.

1: Estimate $\widehat{\mathbb{R}}_{\mathrm{L}}$ by (19) and omit its imaginary part to obtain $\widehat{\mathbb{R}}$ by (23);
2: Compute $\widehat{\mathbb{R}} = \widehat{\mathbb{S}}\widehat{\mathbb{W}}_s\widehat{\mathbb{S}}^T + \widehat{\mathbb{G}}\widehat{\mathbb{W}}_n\widehat{\mathbb{G}}^T$ by (24) to obtain $\widehat{\mathbb{G}}$;
3: Perform search in (25) to get Q candidate angles $\mathbf{\Gamma} = \left\{\widehat{\theta}_1, \widehat{\theta}_2, \cdots, \widehat{\theta}_Q\right\}$;
4: Selected K signal DOAs by $\widehat{\mathbf{\Theta}} = \arg\ \min_{\theta \in \{\mathbf{\Gamma}, -\mathbf{\Gamma}\}} f_{\mathrm{MVDR}}(\theta)$.
5: **return** $\widehat{\mathbf{\Theta}} = \left\{\widehat{\theta}_1, \widehat{\theta}_2, \ldots, \widehat{\theta}_K\right\}$.

4. Complexity analysis

Comparison of primary real-valued computational flops of DOA estimation by various algorithms including the standard MUSIC, C-MUSIC [6] with $\beta = 2$ angular sectors, RV-MUSIC [26], U-MUSIC [19] and the proposed RDRV-MUSIC method are shown in Table 1, where J stands for the total number of spectral sample points over $[-\pi/2, \pi/2]$. Since the main complexity are involved in the EVD step and the spectral search step, flops required by computing the covariance matrix are omitted for all the five algorithms.

The first common term $M^2(K+2)$ included in first four algorithms stands for the real flops costed by computing the EVD of a real matrix of dimensions $M \times M$ by exploiting the fast subspace decomposition (FSD) technique [29]. For the standard MUSIC, since the EVD is performed on the complex matrix $\mathbf{R}$, this term is multiplied by a factor 4. For the proposed method, since $\mathbb{R}$ is a real matrix which is of dimensions $(N+1) \times (N+1)$, this term is reduced to $(N+1)^2(K+2)$.

Table 1
Comparison of real-valued computational flops.

Algorithms	Primary real-valued computations
Standard MUSIC	$4 \times M^2(K+2) + 4 \times J(M+1)(M-K)$
C-MUSIC, $\beta = 2$	$5 \times M^2(K+2) + 4 \times [J(M+1)(M-2K)]$
U-MUSIC	$M^2(K+2) + J(M+1)(M-K)$
RV-MUSIC	$5 \times M^2(K+2) + J(M+1)(M-2K)$
RDRV-MUSIC	$(N+1)^2(K+2) + \frac{1}{2} \times J(N+2)(N+1-K)$

The second common term $J(M+1)(M-K)$ included in first four algorithms indicates the real computational flops costed by computing the spectral amplitudes of J points over $[-\pi/2, \pi/2]$ [3,6,17,26]. For the standard MUSIC, it has to compute all the J spectral points with complex computations, therefore, this term is also multiplied by a factor 4. Since the new method involves a compressed search over only $[0, \pi/2]$ (or $[-\pi/2, 0]$), and $\mathbb{a}(\theta)$ and $\widehat{\mathbb{G}}$ are of reduced dimensions $(N+1) \times 1$ and $(N+1) \times (N+1-K)$, respectively, this term is significantly reduced to $1/2 \times J(N+2)(N+1-K)$.

As a rule, we have $J \gg M > N > K$ [6,7], which means the spectral search dominates the complexity for the four search-based algorithms. Therefore, by using $M = 2N+1$, we have the following approximation

$$\begin{aligned} \frac{C_{RDRV-MUSIC}}{C_{MUSIC}} &\approx \frac{1/2 \times J(N+2)(N+1-K)}{4 \times J(2N+2)(2N+1-K)} \\ &= \frac{1}{32} \cdot \frac{N+2}{N+1} \cdot \frac{N+1-K}{N+(1-K)/2} \\ &\approx \frac{1}{32}. \end{aligned} \tag{27}$$

It follows from (27) that about $31/32 \approx 97\%$ computational flops are dramatically reduced by the new method.

5. Statistical performance study

This section gives a theoretical analysis on the MSE performance of DOA estimate by the new method. The analysis follows directly from the theory of subspace perturbation and Taylor's series expansion [30–34]. Unlike many previous asymptotic performance studies with a sufficiently large number of snapshot, the presented analysis makes an assumption of a high SNR. Under such an assumption, a closed-form expression is derived to predict the MSE of DOA estimation by the proposed method.

The theoretical analysis starts by introducing a $M \times L$ noise-free direct-data matrix $\mathbf{X}$, which is composed of L snapshots of source waveform vectors $\{\mathbf{s}(t)\}_{t=1}^L$ as follows:

$$\mathbf{X} \triangleq \mathbf{A}[\mathbf{s}(1), \mathbf{s}(2), \ldots, \mathbf{s}(L)].$$

The SVD of $\mathbf{X}$ can be written as

$$\mathbf{X} = \mathbf{U}_s\mathbf{\Sigma}_s\mathbf{V}_s^H + \mathbf{U}_n\mathbf{\Sigma}_n\mathbf{V}_n^H, \tag{28}$$

where subscripts s and n denote the signal- and the noise- subspaces, respectively, and $\mathbf{\Sigma}_s$ and $\mathbf{\Sigma}_n$ are two diagonal matrices composed of the K significant- and the $M-K$ zero- singular values of $\mathbf{X}$, respectively [6,26,30–32]. In a noise environment, the ideal $\mathbf{X}$ is perturbed by the additive sensor noise as

$$\widehat{\mathbf{X}} = \mathbf{X} + \mathbf{N} = [\mathbf{x}(1), \mathbf{x}(2), \ldots, \mathbf{x}(L)], \tag{29}$$

where $\mathbf{N} \triangleq [\mathbf{n}(1), \mathbf{n}(2), \ldots, \mathbf{n}(L)]$ is the $M \times L$ matrix of the AWGN. With the AWGN, the noise subspace orthogonal matrices estimated

by the standard MUSIC and that by the proposed algorithm can be written, respectively, as follows:

$$\widehat{\mathbf{G}} = \mathbf{G} + \Delta\mathbf{G}$$
$$\widehat{\mathcal{N}} = \mathcal{N} + \Delta\mathcal{N}.$$

By analyzing the SVD of $\mathbf{X}$, it has been proven that the theoretical perturbation of the original noise subspace orthogonal matrix can be expressed by a linear function of the AWGN matrix $\mathbf{N}$, which is given by the following lemma [30].

Lemma 1: Assume the elements of the AWGN matrix $\mathbf{N}$ are random variables with zero means, then the perturbation of $\widehat{\mathbf{G}}$ at a high SNR can be expressed by a linear function of matrix $\mathbf{N}$ as follows:

$$\Delta\mathbf{G} = -\mathbf{U}_s\boldsymbol{\Sigma}_s^{-1}\mathbf{V}_s^H\mathbf{N}^H\mathbf{U}_n. \tag{30}$$

To establish the distribution of the proposed algorithm and compare it with that of MUSIC, we must give an expression for the theoretical perturbation of the proposed noise subspace $\mathcal{N}$. To this end, we divide matrix $\mathbf{X}$ along its row direction as

$$\mathbf{X} = \begin{bmatrix} \mathbf{X}_1 \\ \cdots\cdots \\ \mathbf{X}_2 \end{bmatrix}.$$

Note that both $\mathbf{X}_1$ and $\mathbf{X}_2$ are of dimensions $(N+1)\times L$. Also note that the elements in the last row of $\mathbf{X}_1$ and those in the first row of $\mathbf{X}_2$ are all ones. Using $\mathbf{X}_1$ and $\mathbf{X}_2$ to define a new matrix $\mathbf{Y}$ as follows:

$$\mathbf{Y} \triangleq \mathbf{J}\mathbf{X}_1 + \mathbf{X}_2,$$

where $\mathbf{J}$ is an $(N+1)\times(N+1)$ exchange matrix with ones on its anti-diagonal and zeros elsewhere. The SVD of $\mathbf{Y}$ can be written as

$$\mathbf{Y} = \mathbf{B}_s\boldsymbol{\Pi}_s\mathbf{C}_s^H + \mathbf{B}_n\boldsymbol{\Pi}_n\mathbf{C}_n^H, \tag{31}$$

where subscripts s and n denote the signal- and the noise- subspaces, respectively, and $\boldsymbol{\Pi}_s$ and $\boldsymbol{\Pi}_n$ are two diagonal matrices composed of the K significant- and the $N+1-K$ zero- singular values of $\mathbf{Y}$, respectively.

As shown in section III that $\mathcal{N}$ can be computed by the EVD of $\mathbb{R}_L$. However, it is difficult to establish the perturbation of $\mathcal{N}$ based on the EVD of $\mathbb{R}_L$. The following theorem indicates that $\mathcal{N}$ can be equivalently obtained by the SVD of $\mathbf{Y}$, and the perturbation of $\mathcal{N}$ can be computed by a linear function of the AWGN matrix $\mathbf{N}$ immediately.

Theorem 1. *Assume the elements of the AWGN matrix* $\mathbf{N}$ *are random variables with zero means, the perturbation of the noise orthogonal matrix* $\mathcal{N}$ *of the proposed RDRV-MUSIC at a high* SNR *can be expressed by a linear function of matrix* $\mathbf{N}$ *as follows:*

$$\Delta\mathcal{N} = \mathbf{D}\mathbf{N}^H\mathcal{N}, \tag{32}$$

where $\mathbf{D} \triangleq -\mathbf{B}_s\boldsymbol{\Pi}_s^{-1}\mathbf{C}_s^H$.

Proof. See Appendix A. □

Using the result of lemma 1 and that of Theorem 1, a closed-form MSE expression for DOA estimation by the proposed RDRV-MUSIC estimator is given by the following theorem.

Theorem 2. *Assume the elements of the AWGN matrix* $\mathbf{N}$ *are random variables with zero means and variance* σ_n^2*, the MSE for the estimation error of incident angle* $\Delta\theta_k \triangleq \widehat{\theta}_k - \theta_k, k \in [1, K]$ *by the proposed RDRV-MUSIC algorithm at a high* SNR *is given by*

$$\mathrm{MSE}_{\mathrm{RDRV-MUSIC}}(\theta_k) = \frac{\sigma_n^2\|\boldsymbol{\alpha}_k\|^2}{|\beta_k|}, \tag{33}$$

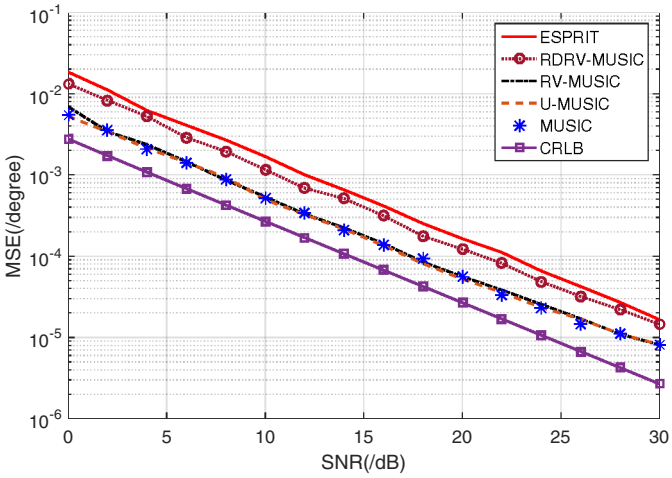

Fig. 3. MSE for $\theta_1 = 30^\circ$ versus high SNRs, $L = 200$ snapshots, 2 sources at $\theta_1 = 30^\circ$ and $\theta_2 = 50^\circ$, half-wavelength ULA, $M = 13$ sensors.

where

$$\boldsymbol{\alpha}_k \triangleq \mathbf{D}^H\mathbb{a}(\theta_k)$$
$$\beta_k \triangleq \mathbb{d}^T(\theta_l)\mathcal{N}\mathcal{N}^H\mathbb{d}(\theta_k)$$

with $\mathbb{d}(\theta_k) \triangleq \partial\mathbb{a}(\theta_k)/\partial\theta_k$ *denoting the first-derivative of* $\mathbb{a}(\theta_k)$ *with respect to* θ_k.

Proof. See Appendix B. □

6. Simulation results

Numerical simulations with 500 independent Monte Carlo trials are conducted to assess the performance of the proposed estimator and to verify the derived MSE expression of DOA estimates by RDRV-MUSIC. For the performance comparison, four algorithms including ESPRIT, MUSIC, RV-MUSIC [26], U-MUSIC [19] and the unconditional Cramér–Rao Lower Bound (CRLB) given in [36] are also applied for references. For all the search-based algorithms including MUSIC, RV-MUSIC , U-MUSIC and the proposed RDRV-MUSIC, a coarse grid 1° was firstly used to get candidate peaks, and a fine one 0.0013° was secondly applied around the candidate peaks for final DOA estimates.

First, we investigate the MSE performance of the proposed method, where high SNRs and large numbers of snapshots are applied. In the simulation, two sources at 30° and 50° are considered, and a half-wavelength ULA composed of 13 sensors with centro-symmetrical geometry is used.

Fig. 3 plots the MSE as functions of the SNR, where high SNRs are considered, which varies over a wide range from 0 dB to 30 dB. It can be concluded from the figure that three algorithms including MUSIC, RV-MUSIC and U-MUSIC have a similar performance to each other, and they show MSEs closest to the CRLB. It can be also seen from the figure that the proposed method has a much better accuracy than ESPRIT, and its MSE tends to the CRLB as the SNR increases. Noting that both the RV-MUSIC and U-MUSIC techniques reduce the complexity by only 75% [6,19] while the proposed estimator saves that by about 97%, the proposed method hence makes an efficient trade-off between computational complexity and estimation accuracy.

To see more clearly the performance of the new approach, Fig. 4 plots MSEs of different algorithms as functions of the number of snapshots, where large numbers of snapshots varying over a wide range from 5×2^5 to 5×2^{14} are exploited. It can be seen again from Fig. 4 that with significantly reduced computational complexity, the proposed technique sacrifices a little estimation accuracy

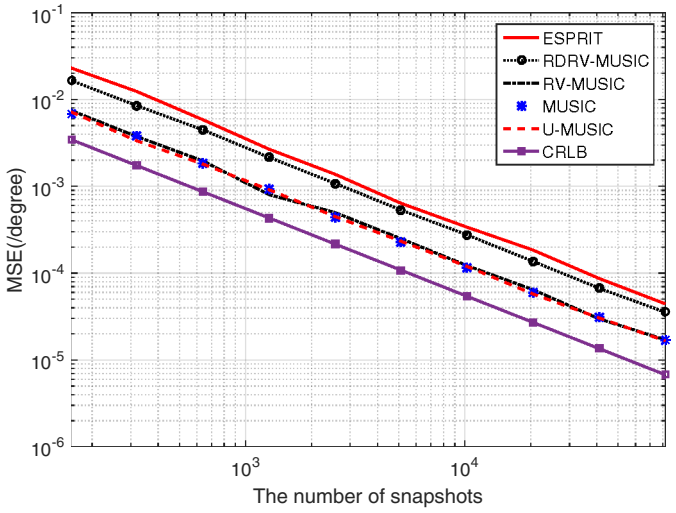

Fig. 4. MSE for $\theta_1 = 30^\circ$ versus large numbers of snapshots, SNR= 0 dB, 2 sources at $\theta_1 = 30^\circ$ and $\theta_2 = 50^\circ$, half-wavelength ULA, $M = 13$ sensors.

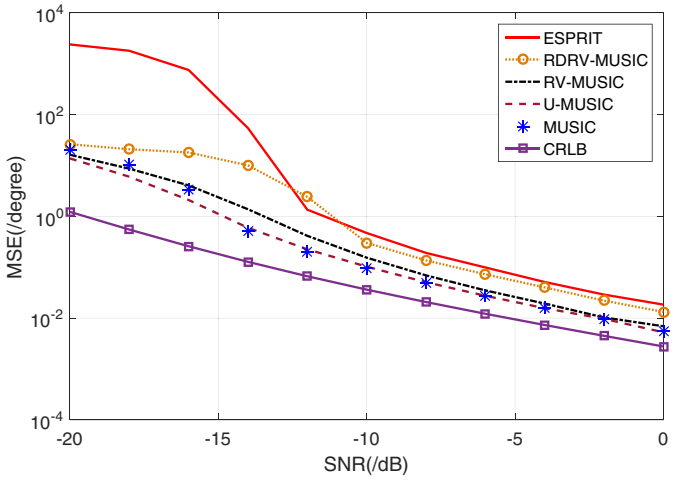

Fig. 5. MSE for $\theta_1 = 20^\circ$ versus low SNRs, $L = 200$ snapshots, 2 sources at $\theta_1 = 20^\circ$ and $\theta_2 = 40^\circ$, half-wavelength ULA, $M = 12$ sensors.

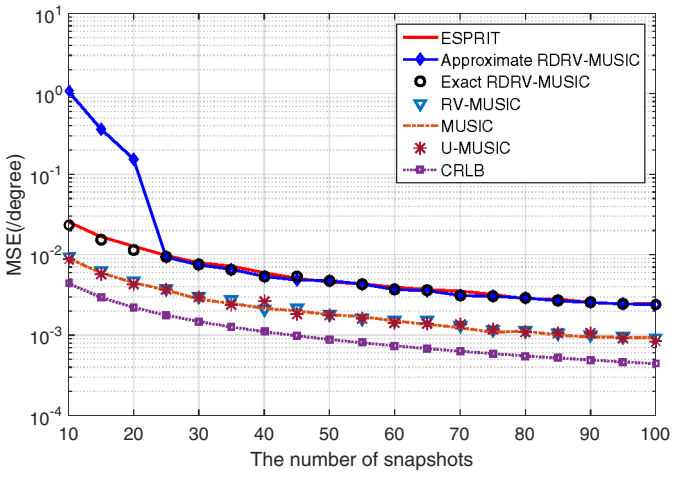

Fig. 6. MSE for $\theta_1 = 20^\circ$ versus small numbers of snapshots, SNR= 0 dB, 2 sources at $\theta_1 = 20^\circ$ and $\theta_2 = 40^\circ$, ULA, $M = 12$ sensors.

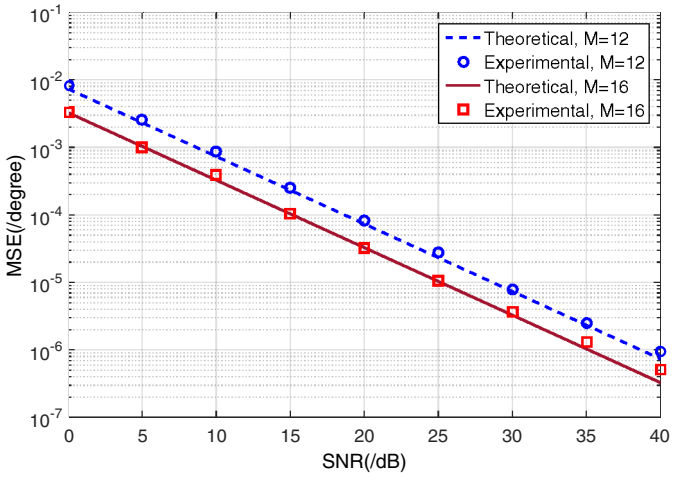

Fig. 7. Theoretical prediction on MSE for $\theta_1 = 30^\circ$ versus the SNRs, $L = 200$ snapshots, 2 sources at $\theta_1 = 30^\circ$ and $\theta_2 = 40^\circ$, tow half-wavelength ULAs with $M = 12$- and $M = 16$ sensors, respectively.

as compared to the three algorithms including MUSIC, RV-MUSIC, U-MUSIC. However, the new method still has a much better MSE than ESPRIT, which tends to the CRLB as the number of snapshot increases.

Second, we examine the performance of the new approach with worse scenarios, where both low SNRs and small numbers of snapshots are considered. Similarly, two sources at 20° and 40° are considered, and a half-wavelength ULA composed of 12 sensors with centro-symmetrical geometry is used in this simulation.

In Fig. 5, the number of snapshots is fixed as $L = 200$ and the SNR is set at a low level, which varies from SNR= −20 dB to SNR= −0 dB. It is seen from the figure that our method shows a significantly improved accuracy as compared to ESPRIT, especially for SNR < -10dB. For SNR > −10 dB, the new method shows a little worse MSE than the standard MUSIC, but it still outperforms ESPRIT.

In Fig. 6, a low SNR = 0 dB as well as small numbers of snapshot varing from $L = 10$ to $L = 100$ are considered. Here, the *exact* RDRV-MUSIC refers to the theoretical cost function $f^{exact}_{\text{RDRV-MUSIC}}(\theta)$ constructed with the complex noise matrix $\mathcal{N}$, as defined in (22). The *approximate* RDRV-MUSIC refers to the practical cost function $f_{\text{RDRV-MUSIC}}(\theta)$ with the real noise matrix $\mathbb{G}$, as defined in (25). It is seen from the figure that the proposed method slightly outperforms ESPRIT with small numbers of snapshots. It is also seen that the proposed RDRV-MUSIC given by $f_{\text{RDRV-MUSIC}}(\theta)$ in fact performs similarly to its theoretical value $f^{exact}_{\text{RDRV-MUSIC}}(\theta)$ with small numbers of snapshots $20 \le L \le 100$. Due to the $\mathcal{O}(1/L)$ dropped error in $\widehat{\mathbb{R}}$, $f_{\text{RDRV-MUSIC}}(\theta)$ shows a worse MSE to $f^{exact}_{\text{RDRV-MUSIC}}(\theta)$ when the numbers of snapshots get sufficiently small as $L \le 20$. Therefore, when sufficiently small numbers of snapshots are available, it is suggested to use $f^{exact}_{\text{RDRV-MUSIC}}(\theta)$ instead of $f_{\text{RDRV-MUSIC}}(\theta)$.

Next, we verify the theoretical MSE expression for DOA estimates by the proposed RDRV-MUSIC algorithm. Note that the theoretical MSEs are computed by (33), which are in fact the predictions of estimation accuracies of $f^{exact}_{\text{RDRV-MUSIC}}(\theta)$ instead of those of $f_{\text{RDRV-MUSIC}}(\theta)$.

Figs. 7 and 8 compare the experimental MSEs with the theoretical ones computed by (33) with different numbers of array elements, where the number of snapshots in Fig. 7 is set as $L = 200$ while that in Fig. 8 varies from a sufficiently small value 5×2^2 to a sufficiently large one 5×2^9. It is seen clearly from the two figures that there is a close match between the simulated results and their theoretical expectations, which verifies the theoretical analysis in Section 5.

Finally, we use a ULA to plot the simulation times of DOA estimates by different algorithms as functions of the number of sen-

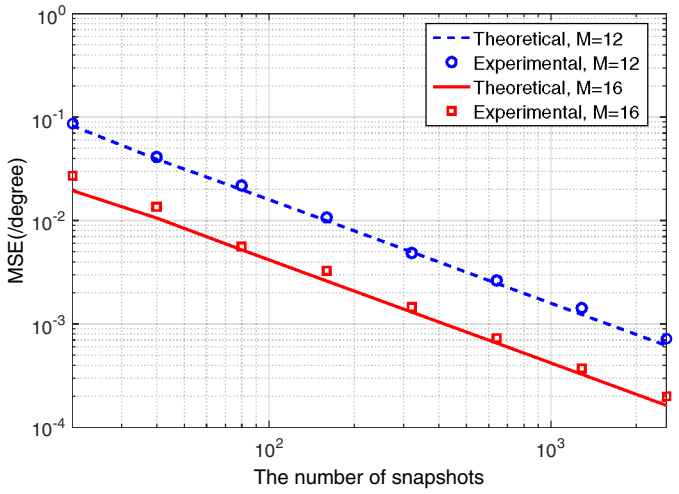

Fig. 8. Theoretical prediction on MSE for $\theta_1 = 30^\circ$ versus the number of snapshots, SNR = 0 dB, 2 sources at $\theta_1 = 30^\circ$ and $\theta_2 = 40^\circ$, tow half-wavelength ULAs with $M = 12$- and $M = 16$ sensors, respectively.

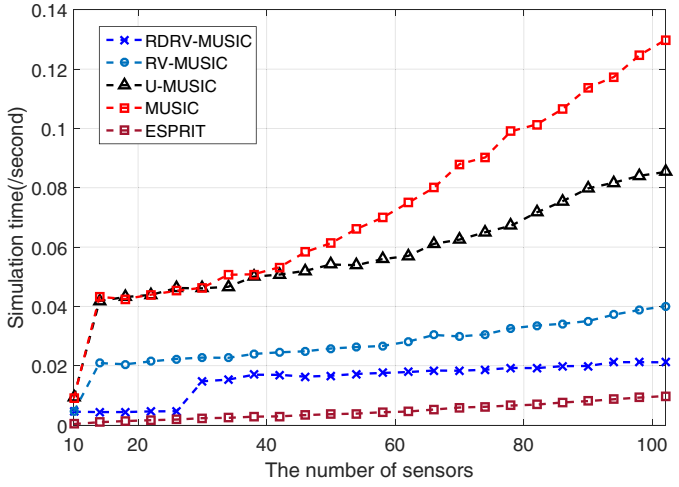

Fig. 9. Simulation time versus the number of sensors, SNR = 0 dB, $L = 100$ snapshots, 2 sources at $\theta_1 = 30^\circ$ and $\theta_2 = 40^\circ$, half-wavelength ULA.

sors in Fig. 9. The simulated results are given by a PC with Intel(R) Core(TM) Duo T5870 2.0 GHz CPU and 1 GB RAM by running the Matlab codes in the same environment. It can be seen from Fig. 9 that the proposed RDRV-MUSIC method is the most efficient one among the four search-based algorithms, which has a significantly smaller simulation time than the other three popular search-based techniques including MUSIC, RV-MUSIC, and U-MUSIC.

7. Conclusions

We have proposed a new computationally efficient algorithm for DOA estimate using a CSA, in which the CSA is divided into two subarrays and the covariance matrices of the two sub-arrays and their cross-correlation ones are exploited to obtain a symmetrical real matrix for a real-valued subspace decomposition. Due to involved real-valued computations and dimension-reduced data with compressed search, the developed method is able to save about 97% complexity as compare to MUSIC. Statistical performance on the MSE of DOA estimation by the new technique and numerical simulations demonstrate that the proposed method is able to provide good accuracy with at low SNRs and with small numbers of snapshots.

Acknowledgment

This work is supported by National Natural Science Foundation of China (61501142), Natural Science Foundation of Shandong Province (ZR2014FQ003), China Postdoctoral Science Foundation (2015M571414), Science and Technology Program of WeiHai and Project Supported by Discipline Construction Guiding Foundation in Harbin Institute of Technology (Weihai) (WH20160107).

Appendix A. Proof of Theorem 1

Comparing (2) and (3) with (13), we have

$$\mathbf{A}_1 = \mathbf{J}\mathbf{A}(1:N+1,:) \tag{A.1-1}$$

$$\mathbf{A}_2 = \mathbf{A}(N+1:M,:). \tag{A.1-2}$$

Hence, the relationships among the original covariance matrix $\mathbf{R}$ and the four ones $\mathbf{R}_{11}$, $\mathbf{R}_{22}$, $\mathbf{R}_{12}$ and $\mathbf{R}_{21}$ are as follows:

$$\mathbf{R} = \begin{bmatrix} \mathbf{J}\mathbf{R}_{11}\mathbf{J}^H & \vdots & \mathbf{J}\mathbf{R}_{12} \\ \cdots & \cdots & \cdots \\ \mathbf{R}_{21}\mathbf{J}^H & \vdots & \mathbf{R}_{22} \end{bmatrix}. \tag{A.2}$$

Combining (7) and (A.2), the estimated matrices $\widehat{\mathbf{R}}_{11}$, $\widehat{\mathbf{R}}_{12}$, $\widehat{\mathbf{R}}_{21}$ and $\widehat{\mathbf{R}}_{22}$ can be written as

$$\widehat{\mathbf{R}}_{11} = \frac{1}{L}\left(\mathbf{J}\widehat{\mathbf{X}}_1\right)\left(\mathbf{J}\widehat{\mathbf{X}}_1\right)^H = \mathbf{J}\widehat{\mathbf{X}}_1\widehat{\mathbf{X}}_1^H\mathbf{J}^H \tag{A.3-1}$$

$$\widehat{\mathbf{R}}_{12} = \frac{1}{L}\left(\mathbf{J}\widehat{\mathbf{X}}_1\right)\widehat{\mathbf{X}}_2^H = \mathbf{J}\widehat{\mathbf{X}}_1\widehat{\mathbf{X}}_2^H \tag{A.3-2}$$

$$\widehat{\mathbf{R}}_{21} = \frac{1}{L}\widehat{\mathbf{X}}_2\left(\mathbf{J}\widehat{\mathbf{X}}_1\right)^H = \widehat{\mathbf{X}}_2\widehat{\mathbf{X}}_1^H\mathbf{J}^H \tag{A.3-3}$$

$$\widehat{\mathbf{R}}_{22} = \frac{1}{L}\widehat{\mathbf{X}}_2\widehat{\mathbf{X}}_2^H. \tag{A.3-4}$$

Substitute x(A.3) into (19), $\widehat{\mathbb{R}}_L$ can be written as

$$\begin{aligned}\widehat{\mathbb{R}}_L &= \widehat{\mathbf{R}}_{11} + \widehat{\mathbf{R}}_{22} + \widehat{\mathbf{R}}_{12} + \widehat{\mathbf{R}}_{21} \\ &= \frac{1}{L}\left(\mathbf{J}\widehat{\mathbf{X}}_1\widehat{\mathbf{X}}_1^H\mathbf{J}^H + \mathbf{J}\widehat{\mathbf{X}}_1\widehat{\mathbf{X}}_2^H + \widehat{\mathbf{X}}_2\widehat{\mathbf{X}}_1^H\mathbf{J}^H + \widehat{\mathbf{X}}_2\widehat{\mathbf{X}}_2^H\right) \\ &= \frac{1}{L}\left(\mathbf{J}\widehat{\mathbf{X}}_1 + \widehat{\mathbf{X}}_2\right)\left(\mathbf{J}\widehat{\mathbf{X}}_1 + \widehat{\mathbf{X}}_2\right)^H \\ &\triangleq \frac{1}{L}\widehat{\mathbf{Y}}\widehat{\mathbf{Y}}^H. \end{aligned} \tag{A.4}$$

In a noise environment, the theoretical $\mathbf{Y}$ is perturbed by the AWGN matrix $\mathbf{N}$ as $\widehat{\mathbf{Y}} = \mathbf{Y} + \mathbf{N}$, and its practical SVD is in fact given by

$$\widehat{\mathbf{Y}} = \widehat{\mathbf{B}}_s\widehat{\mathbf{\Pi}}_s\widehat{\mathbf{C}}_s^H + \widehat{\mathbf{B}}_n\widehat{\mathbf{\Pi}}_n\widehat{\mathbf{C}}_n^H. \tag{A.5}$$

Noting that $L\widehat{\mathbb{R}}_L = \widehat{\mathbf{Y}}\widehat{\mathbf{Y}}^H$, it can be concluded directly by comparing (21) and (A.5) that

$$\widehat{\mathbf{\Pi}}_s^2 = L\widehat{\mathbf{\Omega}}_s, \quad \widehat{\mathbf{B}}_s = \widehat{\mathcal{S}} \tag{A.6-1}$$

$$\widehat{\mathbf{\Pi}}_n^2 = L\widehat{\mathbf{\Omega}}_n, \quad \widehat{\mathbf{B}}_n = \widehat{\mathcal{N}}, \tag{A.6-2}$$

which implies that $\mathcal{N}$ can be also obtained by the SVD of $\mathbf{Y}$ equivalently. Comparing (28) with (31) as well as using (A.6), it can be easily concluded from lemma 1 that the perturbation of the new noise subspace is given by

$$\Delta\mathcal{N} = -\mathbf{B}_s\mathbf{\Pi}_s^{-1}\mathbf{C}_s^H\mathbf{N}^H\mathbf{B}_n = \mathbf{D}\mathbf{N}^H\mathcal{N}, \tag{A.7}$$

which completes the proof. □

Appendix B. Proof of Theorem 4

For the sake of notational simplicity, let us define

$$\boldsymbol{\gamma}_k \triangleq \mathcal{N}\mathcal{N}^H \mathbb{d}(\theta_k)$$
$$\xi_k \triangleq \boldsymbol{\alpha}_k^H \mathbf{N}^H \boldsymbol{\gamma}_k.$$

Using (32) and the zero means of AWGN, it can be easily proven with a high SNR assumption that

$$\lim_{L\to\infty} \widehat{\mathcal{N}}\widehat{\mathcal{N}}^H = \mathcal{N}\mathcal{N}^H. \tag{B.1}$$

Hence, $f_{\text{RDRV-MUSIC}}(\theta)$ is a consistent estimate for θ_k at a high SNR, and we can obtain the second-order approximation of the derivative of $f_{\text{RDRV-MUSIC}}(\theta)$ about the true value θ_k as follows (see [30–35], and references therein)

$$0 \approx f'_{\text{RDRV-MUSIC}}(\theta_k) + \left(\widehat{\theta}_k - \theta_k\right) f''_{\text{RDRV-MUSIC}}(\theta_k), \tag{B.2}$$

where higher-order terms are neglected, and the first- and second-order derivatives of $f_{\text{RV-MUSIC}}(\theta)$ with respect to θ_k are given by

$$f'_{\text{RDRV-MUSIC}}(\theta_k) \triangleq \left.\frac{\partial f_{\text{RDRV-MUSIC}}(\theta)}{\partial\theta}\right|_{\theta=\theta_k}$$
$$f''_{\text{RDRV-MUSIC}}(\theta_k) \triangleq \left.\frac{\partial f'_{\text{RDRV-MUSIC}}(\theta)}{\partial\theta}\right|_{\theta=\theta_k},$$

where the first-order derivative of $f_{\text{RV-MUSIC}}(\theta)$ with respect to θ_k can be specifically expressed as

$$\begin{aligned} f'_{\text{RDRV-MUSIC}}(\theta_k) &= \mathbb{d}^T(\theta_k)\widehat{\mathcal{N}}\widehat{\mathcal{N}}^H \mathbb{a}(\theta_k) \\ &\quad + \mathbb{a}^T(\theta_k)\widehat{\mathcal{N}}\widehat{\mathcal{N}}^H \mathbb{d}(\theta_k). \end{aligned} \tag{B.3}$$

Because $\mathbb{d}^T(\theta_k)\widehat{\mathcal{N}}\widehat{\mathcal{N}}^H\mathbb{a}(\theta_k)$ is a scalar, and noting that $\mathbb{a}(\theta)$ and $\mathbb{d}(\theta)$ are real vectors, we have

$$\begin{aligned} \mathbb{d}^T(\theta_k)\widehat{\mathcal{N}}\widehat{\mathcal{N}}^H\mathbb{a}(\theta_k) &= \left[\mathbb{d}^T(\theta_k)\widehat{\mathcal{N}}\widehat{\mathcal{N}}^H\mathbb{a}(\theta_k)\right]^H \\ &= \mathbb{a}^T(\theta_k)\widehat{\mathcal{N}}\widehat{\mathcal{N}}^H\mathbb{d}(\theta_k). \end{aligned} \tag{B.4}$$

Therefore, the first-order derivative of $f_{\text{RV-MUSIC}}(\theta)$ with respect to θ_k is finally given by

$$f'_{\text{RDRV-MUSIC}}(\theta_k) = 2\mathbb{a}^T(\theta_k)\widehat{\mathcal{N}}\widehat{\mathcal{N}}^H\mathbb{d}(\theta_k). \tag{B.5}$$

Consequently, the second-order derivative of $f_{\text{RV-MUSIC}}(\theta)$ with respect to θ_k can be written as

$$\begin{aligned} f''_{\text{RDRV-MUSIC}}(\theta_k) &= 2\mathbb{d}^T(\theta_k)\widehat{\mathcal{N}}\widehat{\mathcal{N}}^H\mathbb{d}(\theta_k) \\ &\quad + 2\mathbb{a}^T(\theta_k)\widehat{\mathcal{N}}\widehat{\mathcal{N}}^H\mathbb{d}'(\theta_k) \\ &\approx 2\mathbb{d}^T(\theta_k)\widehat{\mathcal{N}}\widehat{\mathcal{N}}^H\mathbb{d}(\theta_k), \end{aligned} \tag{B.6}$$

where the high-order term $\mathbb{a}^T(\theta_k)\widehat{\mathcal{N}}\widehat{\mathcal{N}}^H\mathbb{d}'(\theta_k)$ is neglected in (B.6). Inserting (B.5) and (B.6) into (B.2) and using $\widehat{\mathcal{N}} = \mathcal{N} + \Delta\mathcal{N}$ as well as $\mathbb{a}^T(\theta_k)\mathcal{N} = \mathbf{0}$ leads to the first-order expression for the estimation error $\Delta\theta_k = \widehat{\theta}_k - \theta_k$ as

$$\Delta\theta_k \approx \frac{f'_{\text{RV-MUSIC}}(\theta_k)}{f''_{\text{RDRV-MUSIC}}(\theta_k)} \approx \frac{\mathbb{a}^T(\theta_k)\Delta\mathcal{N}\mathcal{N}^H\mathbb{d}(\theta_k)}{\mathbb{d}^T(\theta_k)\mathcal{N}\mathcal{N}^H\mathbb{d}(\theta_k)}, \tag{B.7}$$

where the second-order term $\mathbb{a}^T(\theta_k)\Delta\mathcal{N}\Delta\mathcal{N}^H\mathbb{d}(\theta_k)$ is neglected in the numerator of (B.7) and $\widehat{\mathcal{N}}\widehat{\mathcal{N}}^H$ in the denominator of (B.7) is replaced by $\mathcal{N}\mathcal{N}^H$ without affecting the performance of estimate $\Delta\theta_k$ (see [30–35] and references therein). Inserting (32) into (B.7), $\Delta\theta_k$ can be simplified as

$$\Delta\theta_k = \frac{\mathbb{a}^T(\theta_k)\mathbf{D}\mathbf{N}^H\mathcal{N}\mathcal{N}^H\mathbb{d}(\theta_k)}{\mathbb{d}^T(\theta_k)\mathcal{N}\mathcal{N}^H\mathbb{d}(\theta_k)} = \frac{\boldsymbol{\alpha}_k^H\mathbf{N}^H\boldsymbol{\gamma}_k}{\beta_k} = \frac{\xi_k}{\beta_k}. \tag{B.8}$$

Thus, the MSE for the estimation error $\Delta\theta_k$ is given by

$$\begin{aligned} \mathrm{E}\left[(\Delta\theta_k)^2\right] &= \frac{\mathrm{E}\left[|\xi_k|^2\right]}{|\beta_k|^2} = \frac{\mathrm{E}\left[\xi_k^H\xi_k\right]}{|\beta_k|^2} \\ &= \frac{\boldsymbol{\gamma}_k^H\mathrm{E}\left[\mathbf{N}\boldsymbol{\alpha}_k\boldsymbol{\alpha}_k^H\mathbf{N}^H\right]\boldsymbol{\gamma}_k}{|\beta_k|^2}. \end{aligned} \tag{B.9}$$

Because $\mathbf{N}\boldsymbol{\alpha}_k$ is a column vector, it can be expanded as a weighted sum of the columns of $\mathbf{N}$. On the other hand, since $\boldsymbol{\alpha}_k^H\mathbf{N}^H$ is a row vector, it can be expanded as a weighted sum of the rows of $\mathbf{N}^H$. Thus, by using the zero means of AWGN, the numerator of (B.9) can written as

$$\begin{aligned} \mathrm{E}\left[|\xi_k|^2\right] &= \boldsymbol{\gamma}_k^H\mathrm{E}\left[\mathbf{N}\boldsymbol{\alpha}_k\boldsymbol{\alpha}^H\mathbf{N}^H\right]\boldsymbol{\gamma}_k \\ &= \boldsymbol{\gamma}_k^H\mathbb{E}\left(\sum_i \alpha_{k,i}\mathbf{n}_i \sum_j \alpha_{k,j}^*\mathbf{n}_j^H\right)\boldsymbol{\gamma}_k \\ &= \boldsymbol{\gamma}_k^H\left[\sum_i\sum_j \left(\alpha_{k,i}\alpha_{k,j}^*\right)\mathrm{E}\left\{\mathbf{n}_i\mathbf{n}_j^H\right\}\right]\boldsymbol{\gamma}_k \\ &= \boldsymbol{\gamma}_k^H\left[\sum_i\sum_j \left(\alpha_{k,i}\alpha_{k,j}^*\right)\delta(i-j)\sigma_n^2\mathbf{I}\right]\boldsymbol{\gamma}_k \\ &= \sigma_n^2\boldsymbol{\gamma}_k^H\|\boldsymbol{\alpha}_k\|^2\boldsymbol{\gamma}_k \\ &= \sigma_n^2\|\boldsymbol{\alpha}_k\|^2\|\boldsymbol{\gamma}_k\|^2, \end{aligned} \tag{B.10}$$

where $\alpha_{k,i}$ and $\alpha_{k,j}$ are the ith and jth element of $\boldsymbol{\alpha}_k$ and $\boldsymbol{\alpha}_k^H$, respectively, $\mathbf{n}_i$ and $\mathbf{n}_j$ and are the ith and the jth column of $\mathbf{N}$, respectively. Substituting (B.10) into (B.9) and using the fact $\|\boldsymbol{\gamma}_k\|^2 = |\beta_k|$, we finally obtain

$$\mathrm{MSE}_{\text{RDRV-MUSIC}}(\theta_l) = \frac{\sigma_n^2\|\boldsymbol{\alpha}_k\|^2}{|\beta_k|}, \tag{B.11}$$

which completes the proof. □

References

[1] J. Krim, M. Viberg, Two decades of array signal processing research: the parametric approach, IEEE Sig. Process. Mag. 13 (3) (1996) 67–94.
[2] J.C. Chen, K. Yao, R.E. Hudson, Source localization and beamforming, IEEE Sig. Process. Mag. 19 (2) (2002) 30–39.
[3] R.O. Schmidt, Multiple emitter location and signal parameter estimation, IEEE Trans. Antennas Propag. AP-34 (3) (1986) 276–280.
[4] F.G. Yan, X.W. Yan, J. Shi, J. Wang, S. Liu, M. Jin, Y. Shen, MUSIC-Like direction of arrival estimation based on virtual array transformation, Sig. Process. 139 (2017) 156–164.
[5] F.G. Yan, M. Jin, X.L. Qiao, Source localization based on symmetrical MUSIC and its statistical performance analysis, Sci. China Inf. Sci. 56 (6) (2013) 1–13.
[6] F.G. Yan, M. Jin, X.L. Qiao, Low-complexity DOA estimation based on compressed MUSIC and its performance analysis, IEEE Trans. Sig. Process 61 (8) (2013) 1915–1930.
[7] M. Rubsamen, A.B. Gershman, Direction-of-arrival estimation for nonuniform sensor arrays: from manifold separation to fourier domain MUSIC methods, IEEE Trans. Sig. Process 57 (2009) 588–599.
[8] F.G. Yan, B. Cao, J.J. Rong, Y. Shen, M. Jin, Spatial aliasing for efficient direction-of-arrival estimation based on steering vector reconstruction, EURASIP J. Adv. Sig. Process (2016) 121.
[9] C. Hao, D. Orlando, G. Foglia, X. Ma, S. Yan, C. Hou, Persymmetric adaptive detection of distributed targets in partially-homogeneous environment, Digit. Sig. Process 24 (2014) 42–51.
[10] C. Hao, D. Orlando, X. Ma, S. Yan, C. Hou, Persymmetric detectors with enhanced rejection capabilities, IET Radar Sonar Nav. 8 (5) (2014) 557–563.
[11] A. De Maio, D. Orlando, An invariant approach to adaptive radar detection under covariance persymmetry, IEEE Trans. Sig.l Process. 63 (5) (2015) 1297–1309.
[12] A. De Maio, D. Orlando, A. Farina, G. Foglia, Design and analysis of invariant receivers for gaussian targets, IEEE J. Sel. Topics Sig. Process. 9 (8) (2015) 1560–1569.
[13] A. De Maio, D. Orlando, C. Hao, G. Foglia, Adaptive detection of point-like targets in spectrally symmetric interference, IEEE Trans. Sig. Process 64 (12) (2016) 3207–3220.
[14] C. Hao, D. Orlando, G. Foglia, G. Giunta, Knowledge-based adaptive detection: joint exploitation of clutter and system symmetry properties, IEEE Sig. Process. Lett. 23 (10) (2016) 1489–1493.

[15] R. Roy, T. Kailath, ESPRIT-Estimation of signal parameters via rotational invariance techniques, IEEE Trans. Sig. Process 37 (7) (1989) 984–995.
[16] B.D. Rao, K.V.S. Hari, Performance analysis of root-MUSIC, IEEE Trans. Acoust. Speech Sig. Process 37 (1989) 1939–1949.
[17] F.G. Yan, Y. Shen, M. Jin, X.L. Qiao, Computationally efficient direction finding using polynomial rooting with reduced-order and real-valued computations, J. Syst. Eng. Electr. 27 (4) (2016) 739–745.
[18] F.G. Yan, Y. Shen, M. Jin, Fast DOA estimation based on a split subspace decomposition on the array covariance matrix, Sig. Process. 115 (2015) 1–8.
[19] K.C. Huarng, C.C. Yeh, A unitary transformation method for angle-of-arrival estiamtion, IEEE Trans. Sig. Process 39 (1991) 975–977.
[20] Z. Guimei, C. Baixiao, Y. Minglei, Unitary ESPRIT algorithm for bistatic MIMO radar, Electr. Lett. 48 (3) (2012).
[21] M. Pesavento, A.B. Gershman, M. Haardt, Unitary root-MUSIC with a real-valued eigendecomposition: a theoretical and experimental performance study, IEEE Trans. Sig. Process 48 (5) (2000) 1306–1314.
[22] A.B. Gershman, P. Stoica, On unitary and forward-backward MODE, Digit. Sig. Process 9 (2) (1999) 67–75.
[23] N. Yilmazer, J. Koh, T.K. Sarkar, Utilization of a unitary transform for efficient computation in the matrix pencil method to find the direction of arrival, IEEE Trans. Sig. Process 54 (2006) 175–181.
[24] D.A. Linebarger, R.D. DeGroat, E.M. Dowling, Efficient direction-finding methods employing forward-backward averaging, IEEE Trans. Sig. Process 42 (8) (1994) 2136–2145.
[25] M. Haardt, J.A. Nossek, Unitary ESPRIT: how to obtain increased estimation accuracy with a reduced computational burden, IEEE Trans. Sig. Process. 43 (5) (1995) 1232–1242.
[26] F.G. Yan, M. Jin, S. Liu, X.L. Qiao, Real-valued MUSIC for efficient direction estimation with arbitrary array geometries, IEEE Trans. Sig. Process 62 (6) (2014) 1548–1560.
[27] F.G. Yan, T. Jin, M. Jin, Y. Shen, Subspace-based direction-of-arrival estimation using centro-symmetrical arrays, Electr. Lett. 27 (11) (2016) 1895–1896.
[28] J. Capon, High-resolution frequency-wavenumber spectrum analysis, in: Proc. IEEE, vol. 57, 1987, pp. 1408–1418.
[29] Xu, Kailath, Fast subspace decomposition, IEEE Trans. Sig. Process. 42 (3) (1994) 539–551.
[30] F. Li, R.J. Vaccaaro, Analysis of min-norm and MUSIC with arbitrary array geometry, IEEE Trans. Aerosp. Electron. Syst. 26 (6) (1990) 976–985.
[31] F. Li, H. Liu, R.J. Vaccaro, Performance analysis for doa estimation algorithms: unification, simplification, and observations, IEEE Trans. Aerosp. Electron. Syst. 29 (4) (1993) 1170–1184.
[32] P. Stoica, K.C. Sharman, Maximum likelihood methods for direction-of-arrival estimation, IEEE Trans. Acoust. Speech Sig. Process. 38 (7) (1990) 1132–1143.
[33] P. Stoica, T. Soderstrom, Statistical analysis of a subspace method for bearing estimation without eigendecomposition, Proc. Inst. Electr. Eng. F. 139 (4) (1992) 301–305.
[34] J. Xin, A. Sano, Computationally efficient subspace-based method for direction-of-arrival estimation without eigendecomposition, IEEE Trans. Sig. Process 52 (4) (2004) 876–893.
[35] P. Stoica, T. Soderstrom, Statistical analysis of a subspace method for bearing estimation without eigendecomposition, in: Proc. IEE., volume 139, 1992, pp. 301–305. Pt. F.
[36] P. Stoica, A. Nehorai, Performance study of conditional and unconditional direction-of-arrival estimation, IEEE Trans. Acoust. Speech Sig. Process. 38 (1990) 1783–1795.